

The characterization of the fluorescence of L-histidine in simulated body fluid

M.O. Iwunze*

Department of Chemistry, Morgan State University, Baltimore, MD 21251, United States

Received 2 May 2005; received in revised form 13 May 2006; accepted 19 May 2006

Available online 1 September 2006

Abstract

In addition to being an essential natural amino acid, L-histidine is biologically important in the dismutation of superoxide radical ($O_2^{\bullet-}$) by superoxide dismutase (SOD). In this work, fluorescence and absorptiometric techniques were used to characterize the photo-phenomenon and optical properties of this compound in a simulated body fluid (SBF). L-Histidine fluoresces at 360 nm when excited at 220 nm. Its molar absorptivity, ϵ , is $4.8 \times 10^3 \text{ M}^{-1} \text{ cm}^{-1}$. The observed bimolecular quenching rate constant, k_q , of $7.5 \times 10^8 \text{ M}^{-1} \text{ s}^{-1}$, by hydrogen peroxide, suggests a non-diffusional activation-controlled mechanism with a rate constant, k_a , of $8.55 \times 10^8 \text{ M}^{-1} \text{ s}^{-1}$ and an electron transfer rate constant, k_{ET} of $6.06 \times 10^8 \text{ s}^{-1}$. The determined radiative and non-radiative rate constants, 4.73×10^7 and $2.9 \times 10^8 \text{ s}^{-1}$, respectively, suggests that the deactivation of the thermally excited L-histidine is by non-radiative route rather than by normal fluorescence, which accounts for the low quenching constant, K_{SV} , of 2.22 M^{-1} that was obtained. The solvent reorganization energy, λ_s , and the reaction free energy change, ΔG , of 1.48 and -5.62 eV , respectively, suggest that the electron transfer reaction in the L-histidine– H_2O_2 reaction is through a solvent separated mechanism.

© 2006 Elsevier B.V. All rights reserved.

Keywords: Fluorescence; L-Histidine; Simulated body fluid; Activation-controlled; Solvent reorganization energy

1. Introduction

L-Histidine is one of the naturally occurring amino acids. It plays a very active role in many biological systems [1–3]. Its relevance in the overall structure and activity of the metalloenzyme, superoxide dismutase (SOD), in the dismutation of debilitating superoxide is well documented [4–7]. The nitrogens on the imidazole moiety of this amino acid, which is a vital component of superoxide dismutase, is ligated to copper and zinc ions as shown in Fig. 1. These metallic sites act as the catalytic centers for the superoxide dismutation reactions. In order to fully understand the mechanism by which this amino acid performs its multifarious biological functions, its optical and physico-chemical properties must be known and be controllable for more efficient tailoring of its activities for specific functions.

Fluorescence techniques have always been found to be quite sensitively reliable in its application in the study and the understanding of chemical and biological reactions. Data obtained by

fluorescence techniques have been found reliable in obtaining not only the binding constants between molecules but also in the determination of the rate of such binding as well as the resulting mechanism. This is especially important in the binding of bio-molecules to enzymes for catalysis in bio-activities [8–16]. Fluorescence quenching studies have been used extensively in this type of studies. We have therefore carried out fluorescence quenching experiments of L-histidine using hydrogen peroxide as a quencher molecule, in order to obtain vital physico-chemical and optical properties of this compound.

SOD is a cytosolic metalloenzyme and its reactions are carried out in that medium. Therefore, in order to obtain spectrochemical properties that is meaningfully consistent with what is obtained in the cytosol, spectrochemical experiments were conducted in a simulated body fluid (SBF) that is known to efficiently mimic biological fluid [17]. The observed pH of the SBF medium used in this work is 7.4, which is very close to the biological pH. In this medium and at this pH, L-histidine exists essentially as a neutral compound as shown in Fig. 2. Its isoelectronic point (pI) at this pH is known to be about 7.5 [18], which is in close agreement with the pH of the SBF medium used in this work.

* Tel.: +1 443 885 3634; fax: +1 443 885 8286.

E-mail address: muwunze@jewel.morgan.edu.

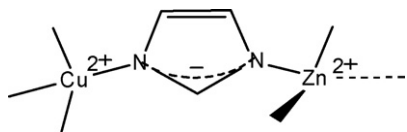


Fig. 1. Structure of the imidazole moiety of L-histidine showing the ligated metal ions on the nitrogen atoms.

2. Experimental

2.1. Chemicals

ACS certified grade L-histidine was obtained from J.T. Baker so also is a 99.0% purity quinine sulfate. A 30.7% analytical reagent grade hydrogen peroxide and a 95–98% pure sulfuric acid were obtained from Sigma–Aldrich. Cetyltrimethylammonium bromide (CTAB) (99.0% purity), magnesium chloride (99.0% pure) and ACS reagent grade disodium phosphate (Na_2HPO_4) were obtained from Acros. Potassium chloride (99.4% pure), calcium chloride (99.0% pure) and sodium bicarbonate (NaHCO_3) (~100.0% pure) were obtained from Fisher chemicals and sodium chloride of 99.98% purity was obtained from Thorn Smith chemist. All chemicals were used as received.

2.2. Simulated body fluid preparation

This fluid system which was used as the solvent for all experiments performed in this work was prepared in accordance with literature directions [19,20]. Briefly, the following compounds were dissolved in 500 mL of triply distilled deionized water: NaCl (3.9681 g); KCl (0.1864 g); CaCl_2 (0.1387 g); MgCl_2 (0.1307 g); NaHCO_3 (0.1764 g) and Na_2HPO_4 (0.0710 g). These compounds give an ionic concentration of Na^+ (143 mM), K^+ (5.0 mM), Mg^{2+} (1.5 mM), Ca^{2+} (2.5 mM), Cl^- (148.8 mM), HCO_3^- (4.2 mM), and HPO_4^- (1.0 mM). The ionic strength was calculated to be 0.16 M and the pH of the solution is about 7.4.

2.3. Optical measurements

All fluorescence measurements were performed using a Perkin-Elmer's Luminescence Spectrophotometer, Model LS 50B. The L-histidine exhibits complex fluorescence spectra due to the presence of the imidazole moiety [21]. For this reason the excitation and emission wavelength of this compound were determined by varying the excitation wavelength from 200 to 250 nm and observing the resulting fluorescence intensity. This

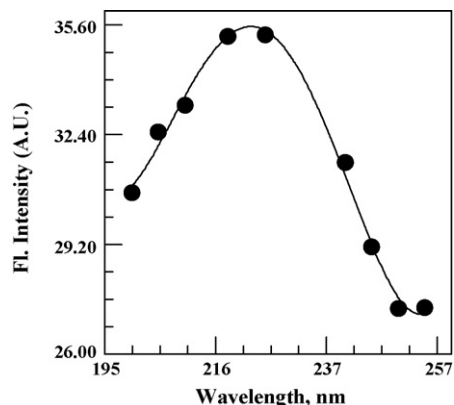


Fig. 3. Plot of the observed fluorescence intensity of L-histidine as a function of the exciting wavelength.

way the excitation wavelength that gave the maximum emission intensity was obtained at 220 nm as can be seen in Fig. 3. The wavelength (220 nm) was used for all further excitation experiments in this work. The excitation and emission slits were kept constant at 3.0 nm. At this excitation wavelength, the fluorescence of this amino acid was observed at 360 nm. In all experiments, unless otherwise specified, the concentration of L-histidine was kept constant at 2.5×10^{-4} M and the concentration of the quencher, hydrogen peroxide, was varied from 0.0185 to 0.1294 M. All experiments were conducted at room temperature (25 ± 0.2 °C). The fluorescence spectra from which the fluorescence intensities were obtained were uncorrected.

The absorptiometric experiments were performed using a Cary Spectrophotometer, Model 1E, supplied by Varian Analytical Instruments. Absorptiometric spectrum of this compound whose λ_{max} is observed at 211 nm was also obtained using a 1.0 cm cuvette. This absorption wavelength of L-histidine is in good agreement with that observed by Tatischeff et al. [21]. The molar absorptivity, ϵ , of L-histidine in SBF was determined by plotting the ratio of the observed absorbance, A , taken at λ_{max} to the concentration, C , as a function of the respective wavelengths encompassing the absorbance spectrum in accordance with Beer–Lambert's law (A/bC). b is the solution thickness or light path length, was 1.0 cm. The ϵ was taken at the peak of the plot at which $\lambda = \lambda_{\text{max}}$.

2.4. Refractive index determination

The refractive index, n , of SBF and 0.05 M H_2SO_4 solutions were determined using the digital Abbe Leica Refractometer

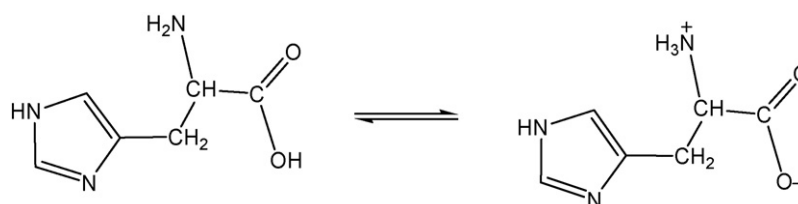


Fig. 2. Structure of L-histidine at isoelectric point (pI) of 7.59.

which was calibrated with a triply distilled deionised water. The obtained refractive indices for these solutions were 1.33563 and 1.33336, respectively.

2.5. Quantum yield

The quantum yield, Φ , of L-histidine was determined in accordance with the literature methodology [22]. Briefly, the solutions of the reference standard (quinine sulfate) and the L-histidine were prepared to have approximately equal absorbance, 0.0304 and 0.0321, respectively, and both were excited at the same wavelength (223.0 nm). In a review articles on quantum yields determination, Demas and Crobby [23] comment that the quantum yield of quinine sulfate is constant between the excitation wavelength of 200 and 390 nm. The value of the quantum yield for this reference sample is recommended to be 0.54 and it was used in this work. This way, the fluorescence emission spectrum of the L-histidine solution was corrected for quantum yield determination. The observed absorbance and fluorescence were further corrected in accordance with Eq. (1) [24]:

$$\Phi_u = \Phi_s \frac{(1 - 10^{-A_s})F_u n_u^2}{(1 - 10^{-A_u})F_s n_s^2} \quad (1)$$

In this equation, the subscripts u and s refer to the unknown sample (L-histidine in SBF) and reference sample (quinine sulfate), respectively. The A and F refer to the absorbance and area of the fluorescence band, respectively. Using the above equation, the fluorescence quantum yield for L-histidine was determined as 0.14. This value is in good qualitative agreement with the quantum yield values of some aromatic amino acids [25,26].

2.6. Fluorescence lifetime

The fluorescence lifetime, τ_0 , for L-histidine in SBF was determined using the Strickler–Berg relation [27] given in Eq. (2):

$$\frac{1}{\tau_0} = 2.88 \times 10^{-9} n^2 \nu_f^3 \phi^{-1} \int \varepsilon d \ln \nu \quad (2)$$

In this equation n , ν_f and ν are the solvent (SBF) refractive index, the fluorescence wave number, taken at the center of gravity of the fluorescence spectrum, and the integrated wave number of the absorption band, respectively. L-Histidine exhibits an uncomplicated single absorption band whose maximum centered at 211 nm. The integration in Eq. (2) was therefore done analytically by measuring of the area enclosed under the absorbance envelope using the relation of full width at half maximum (FWHM) technique. In this case Eq. (2) is reduced to a much simpler relation given in Eq. (3):

$$\frac{1}{\tau_0} = 2.88 \times 10^{-9} n^2 \nu_f^3 \phi^{-1} \varepsilon \ln \left(\frac{\nu_2}{\nu_1} \right). \quad (3)$$

Subscripts 1 and 2 in this equation denote the wavenumber corresponding to the high and low end of the wavenumbers of the band.

2.7. Electrochemical experiment

Cyclic voltammetric technique performed with an Electrochemical Analyzer supplied by Cypress Systems was used to obtain the current–voltage data with which the $E_{1/2}$ value for L-histidine was determined. The working electrode in this experiment was a glassy carbon electrode of 0.016 cm² electrochemical surface area. The counter and quasi-reference electrodes were a wound platinum wire and a silver rod, respectively. L-Histidine is known to be electro-inactive in aqueous solution [28]; therefore the oxidation peak potential, E_p , was obtained in a 0.01 M cationic (cetyltrimethylammonium bromide) micellar solution. In all solutions, 0.15 M KCl was used as supporting electrolyte and in each solution a fairly constant value of 1.48 V versus SCE was obtained. The concentration of L-histidine in all the solutions was 3.66×10^{-3} M.

3. Results and discussion

Fig. 4 is the L-histidine absorbance spectrum with which the fluorescence lifetime, τ_0 , and molar absorptivity, ε , of 4.8×10^3 M⁻¹ cm⁻¹ were obtained, as described in Section 2.3. The spectra of the steady state fluorescence experiments of L-histidine in SBF at different concentrations of hydrogen peroxide and at a constant L-histidine concentration are shown in Fig. 5. As indicated by the arrow in this figure, the fluorescence intensity of L-histidine is seen to decrease with increasing hydrogen

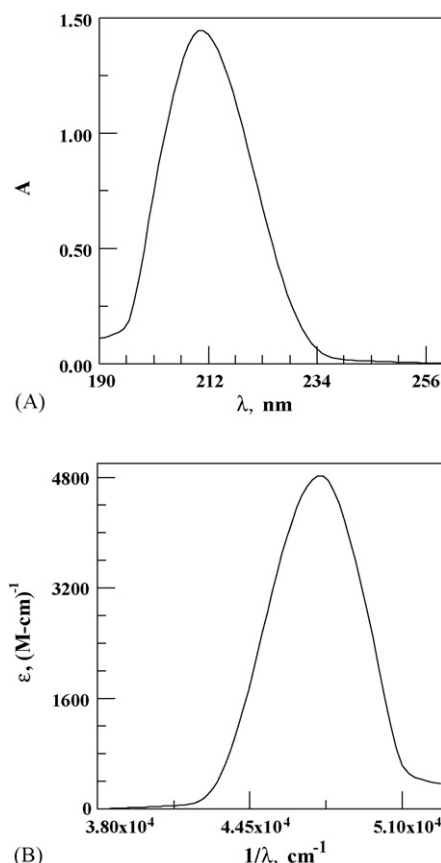


Fig. 4. The absorbance spectrum of L-histidine.

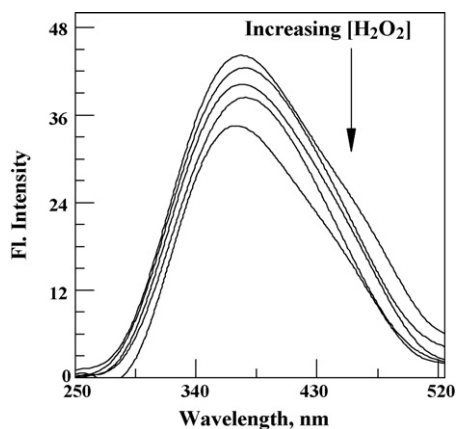


Fig. 5. The fluorescence spectra of L-histidine with increasing concentration of hydrogen peroxide (see text).

peroxide (quencher, Q) concentration, as it should be. Analysis of the quenching data was carried out in accordance with the Stern–Volmer relationship as given in Eq. (4):

$$\frac{I^0}{I} = 1 + K_{SV}[\text{H}_2\text{O}_2] = 1 + k_q\tau_0[\text{H}_2\text{O}_2] \quad (4)$$

I^0 and I in this equation are the observed fluorescence intensity in the absence and in the presence of quencher, respectively. The values of I^0 and I were taken at the emission band maximum as is usually the standard practice. K_{SV} is the Stern–Volmer quenching constant and k_q and τ_0 are the quenching rate constant and the natural fluorescence lifetime of L-histidine, respectively. The plot of the observed data, in accordance with Eq. (4) is shown in Fig. 6. As can be seen, the plot obeyed the Stern–Volmer equation with a correlation coefficient of better than 0.99 with a slope of 2.22 M^{-1} , corresponding to K_{SV} as per Eq. (4). This value was used with the value of τ_0 discussed above, to obtain a quenching rate constant, k_q , of $7.5 \times 10^8 \text{ s}^{-1}$. The observed experimental and calculated parameters for this work are listed in Table 1. As can be seen the value of K_{SV} is surprisingly low and may be explained by the deactivation of the thermally excited L-histidine via non-radiative route. It has been established that

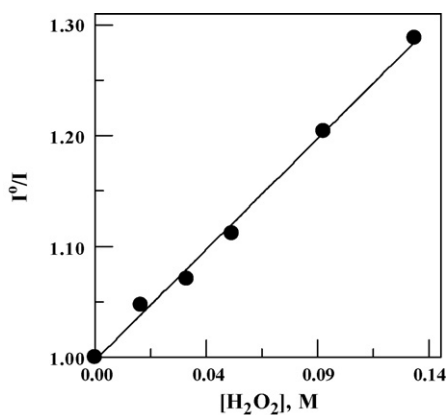


Fig. 6. The Stern–Volmer plot of L-histidine with hydrogen peroxide as quencher.

Table 1

The observed and calculated physico-chemical and optical properties of L-histidine in SBF

| Parameter | Value | Parameter | Value |
|------------------------|--|------------------------|---|
| ϵ | $4.8 \times 10^3 \text{ M}^{-1} \text{ cm}^{-1}$ | λ_{exc} | 220 nm |
| λ_{max} | 211 nm | λ_{em} | 360 nm |
| Φ | 0.14 | τ_0 | 2.96 ns |
| k_r | $4.73 \times 10^7 \text{ s}^{-1}$ | $K(R)$ | 1.48 |
| k_{nr} | $2.9 \times 10^8 \text{ s}^{-1}$ | k_q | $7.5 \times 10^8 \text{ M}^{-1} \text{ s}^{-1}$ |
| k_a | $8.55 \times 10^8 \text{ M}^{-1} \text{ s}^{-1}$ | k_{ET} | $6.06 \times 10^8 \text{ s}^{-1}$ |
| ΔG° | -5.62 eV | $\Delta\lambda_s$ | 1.48 eV |
| k_d | $6.11 \times 10^9 \text{ M}^{-1} \text{ s}^{-1}$ | K_{SV} | 2.22 M^{-1} |

H_2O_2 is a good electron scavenger [29,30] and can interact with the thermally excited L-histidine at the excited state and form a charge transfer complex at the excited state. It is further noted by these authors that no ground state complexation was formed between hydrogen peroxide and the compounds studied. That argument is consistent with what is observed in this work.

As can be seen in Fig. 5, there is no apparent structural difference between the fluorescence spectrum of L-histidine in the presence and the absence of H_2O_2 . This signifies that there is no ground state complexation between this fluorophore and the quencher to account for the low K_{SV} observed in this work. It is further observed (Fig. 5) that at the excited state the H_2O_2 can withdraw electron from the fluorescer, L-histidine. When this happens, the H_2O_2 becomes an ineffective quencher and the L-histidine can thereafter return to ground electronic level via non-radiative route. This type of mechanism has been reported by several workers with respect to some aromatic amino acids and indole derivatives [29–33]. This deactivation route, non-radiative decay by excited L-histidine can account for the low K_{SV} obtained in this work. Furthermore, a comparison of the radiative and non-radiative deactivation rate constants can be used to lend credence to the observed low K_{SV} :

$$k_r = \frac{\Phi}{\tau_0} \quad (5)$$

$$k_{\text{nr}} = \frac{1 - \Phi}{\tau_0} \quad (6)$$

In the above equations, k_r and k_{nr} are radiative and non-radiative rate constants and the rest terms have the meanings described earlier. Using the observed values of 0.14 and 2.96 ns for Φ and τ_0 , respectively, the k_r and k_{nr} values determined were 4.73×10^7 and $2.9 \times 10^8 \text{ s}^{-1}$, respectively. From these values it can be seen that the deactivation rate constant of the thermally excited L-histidine due to non-radiative process, k_{nr} , is about an order of magnitude more than that of pure fluorescence, k_r . These observed rate constants may be used as a further suggestion that the deactivation of the thermally excited L-histidine is by non-radiative route rather than by normal fluorescence, and this fact can account for the low quenching constant, K_{SV} that was obtained as discussed above. The obtained k_q was compared with the theoretical bimolecular diffusion-controlled reaction rate constant, k_d , using the Smoluchowski–Debye equation for neutral reacting species such as those under consideration in

this work:

$$k_d = \frac{4\pi N}{100(D_A + D_D)(R_A + R_D)} \quad (7)$$

D and R in this equation refer to diffusion coefficient and radius, respectively, and N is the Avogadro number. Subscripted A and D refer to acceptor and donor species, hydrogen peroxide and L-histidine, respectively. The radius, R , values were obtained using the Smoluchowski relation: $R = (3M/4\pi N\rho)^{1/3}$, where M and ρ refer to the molar mass and the density of the respective compounds. The ρ for hydrogen peroxide (1.11 g cm^{-3}) was taken from Ref. [34], giving R -value of $2.30 \times 10^{-8} \text{ cm}$. The ρ for L-histidine (1.42 g cm^{-3}) from which an R -value of $3.51 \times 10^{-8} \text{ cm}$ was determined was obtained from the ACD/lab extension program of the CS ChemDraw of the CambridgeSoft Corporation, Version 6.0 [35]. The density thus obtained is in agreement with what is reported in the J.T. Baker MDS sheet for this amino acid and also with that calculated using the incremental atomic volume method by Edwards [36]. The diffusion coefficient for the reactants was calculated using the Stokes–Einstein relationship ($D = kT/6\pi\eta R$), where k is the Boltzmann constant, η the viscosity of the medium (SBF) (1.13 cP) and $T = 298 \text{ K}$. The value of k_d obtained from these relations is $6.11 \times 10^9 \text{ M}^{-1} \text{ s}^{-1}$. This value is an order of magnitude larger than the k_q value given above. This indicates that the reaction between L-histidine and hydrogen peroxide is not diffusion controlled.

3.1. Electron transfer rate constant

As stated earlier in Section 3, the K_{SV} that was obtained in this work is quite low and that the deactivation reaction is considered to be due to a non-radiative process. Further probing of the mechanism for the observed quenching reaction was considered. According to Sutin [37], k_q and k_d are related to the electron transfer constant, k_{ET} , by the equation:

$$k_q = \frac{k_{ET}k_d}{k_{ET} + k_{-d}} \quad (8)$$

k_{-d} in this equation is the first order diffusion-controlled dissociation rate constant of the precursor complex shown in the following scheme:



Rearrangement of Eq. (8), in accordance with Darocher's method [38], gives the following:

$$\frac{1}{k_q} = \frac{1}{k_d} + \frac{k_{-d}}{k_{ET}k_d} = \frac{1}{k_d} + \frac{1}{K(R)k_{ET}} \quad (9)$$

k_{ET} is the first-order electron transfer rate constant and $K(R)$ (equal to k_d/k_{-d}) is the distant dependent association or equilibrium constant of the precursor complex that is obtained using the Debye and Fuoss–Eigen model [39–41] given in Eq. (8) for uncharged reactants as is the case in this work:

$$K(R) = \frac{4\pi NR^3}{3000} \quad (10)$$

The value of $K(R)$ thus calculated is 1.48 M^{-1} , when the R -value is approximated by the sum of the radii of the reactants (5.81 \AA). A combination of Eqs. (6)–(8) was used to obtain k_{ET} of $6.06 \times 10^8 \text{ s}^{-1}$. This value is consistent with what is expected for long range photo induced electron transfer reactions within an encounter radius $\geq 7 \text{ \AA}$ [42–45]. The activation-controlled rate constant, k_a , of $8.55 \times 10^8 \text{ s}^{-1}$ for the reaction under study was determined using the Sutin formalism [37]: $k_a = K(R)k_{ET}$. These rate constants are listed in Table 1. A comparison of the magnitude of k_a with k_q , k_d and k_{ET} reveals some relevant facts in this work: (a) $k_q = k_a$ and $k_{ET} < k_d$ and (b) K_{SV} is quite low. The observation in (a) implies an activation-controlled reaction process and the observed k_{ET} is within a value expected in a solvent separated radical ion pair reaction.

3.2. Solvent reorganization energy

In order to fully understand the observed electron transfer mechanism, the solvent involvement is considered. For the calculation of the solvent reorganization energy, λ_s , we have used the Marcus dielectric continuum formula [46] given in Eq. (11):

$$\lambda_s = \frac{e^2}{4\pi\epsilon_0(1/\epsilon_{0,p}^2 - 1/\epsilon_s)(1/2R_A + 1/2R_D - 1/R_{AD})} \quad (11)$$

In the above equation $\epsilon_{0,p}$ ($\epsilon_{0,p} = n^2$) and ϵ_s are the solvent refractive index and the solvent dielectric constant, respectively. The value of $\epsilon_{0,p}$ (1.7839) was experimentally determined as described in Section 2.4. The observed refractive index of the SBF is within the value of the dioxane–water mixture whose dielectric constant from 10 to 100% dioxane is known [47]. The estimation of fluidic dielectric constant based on dioxane–water scale is frequently used in experimental works [48–54]. Therefore the dielectric constant of SBF was estimated from this scale and was found to be 78.3 D. This can be compared to that of water, which is known to be 78.355 D [55]. This is not surprising since the SBF is essentially a water-solution of different ionic species as shown in Section 2.2. In Eq. (11), e is the electronic charge and ϵ_0 is the permittivity of vacuum. The use of this equation gave a value of 1.48 eV for the solvent reorganization energy for L-histidine– H_2O_2 reaction in SBF. The observed λ_s value is within the range of those values that implicate a solvent separated reaction process.

3.3. Free energy change

In addition to the solvent reorganization energy, the free energy change, ΔG° , for the electron transfer reaction in this system was also determined using the Rehm–Weller relationship given in Eq. (12) [56,57]:

$$\Delta G^\circ = E_{1/2}^\circ - E_{1/2}^r - E_{0-0} - \frac{e^2}{4\pi\epsilon_0\epsilon_s R_q} \quad (12)$$

In this equation $E_{1/2}^\circ$ and $E_{1/2}^r$ are the half-wave potentials of the oxidant and reductant species of the reactants, H_2O_2 and L-histidine, respectively. E_{0-0} is the zero–zero excitation energy of L-histidine taken at the maximum of the excitation spectrum.

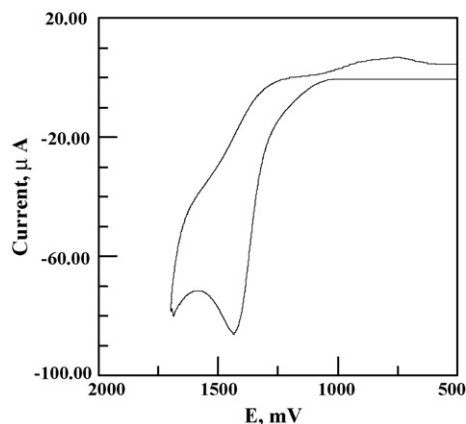


Fig. 7. The voltammogram of 3.015×10^{-3} M L-histidine at glassy carbon electrode in 0.01 M cationic surfactant (CTAB) Micelle and 0.15 M KCl as supporting electrolyte.

R_q is the effective electron transfer encounter distance between the reactants, which is related to the observed quenching rate constant by Eq. (13) [58]:

$$k_q = 4\pi N' D_{AD} R_q \quad (13)$$

However, in this work, the R_q (7.51×10^{-8} cm) in the above equation was approximated to $R_A + R_D + R_{\text{solvent}}$, where the R_{solvent} is the radius of the water molecule sandwiched between the reactants, as it is observed that the reactants in the reaction under study are solvent separated as observed in Section 3.2.

3.4. Determination of the oxidation peak potential of L-histidine

Cyclic voltammogram of L-histidine was obtained as described in Section 2. This is shown in Fig. 7. As can be seen from this voltammogram, L-histidine exhibited a non-reversible behavior and the peak potential is centered at about 1.48 V. As a result of the irreversibility of this compound, the half-wave potential is difficult of ascertain without some ambiguity. As an approximation, therefore the peak potential was used in place of the half-wave potential given in Eq. (12). This was also the case for the hydrogen peroxide whose peak potential of 1.76 V versus NHE was taken from Refs. [59,55]. This value is in good agreement with other literature value [54]. The determined peak potential of L-histidine was referenced to the NHE scale before its use for the determination of ΔG° . Using these values, the ΔG° was calculated as -5.62 eV. This very high exergonic free energy value is well within the value consistent with a solvent-separated (or outer sphere) reaction mechanism [60–62].

4. Conclusion

It has been shown in this work that L-histidine is excitable at a wavelength of 220 nm and its fluorescence is observed at 360 nm. Its absorption wavelength and molar absorptivity were determined as 211 nm and $4.8 \times 10^3 \text{ M}^{-1} \text{ cm}^{-1}$, respectively. Its bimolecular reaction with hydrogen peroxide is not diffusion-limited but rather an activation-controlled process. Its

deactivation is also not through a normal fluorescence decay but through a non-radiative process. Both of the reorganization energy, λ_s , and the free energy change of the reaction, ΔG° , implies further that the reaction is consistent with a solvent separated ion pair mechanism.

Acknowledgement

The author is grateful to the Extramural Associates Research Development Award (ERDA) of National Institute of Health/Morgan State University for support of this work.

References

- [1] R.H. Hol, P. Kennepohl, E.I. Solomon, *Chem. Rev.* 96 (1996) 2239–2314.
- [2] S. Karlin, Z.Y. Zhu, K.D. Karlin, *Proc. Natl. Acad. Sci. U.S.A.* 94 (1997) 14225–14230.
- [3] J.A. Roe, et al., *Biochemistry* 27 (1988) 950–958.
- [4] J.A. Tainer, et al., *J. Biol. Chem.* 160 (1982) 181–217.
- [5] J.A. Tainer, et al., *Nature* 306 (1983) 284–287.
- [6] M.A. High, S.S. Hasnain, *J. Mol. Biol.* 287 (1999) 579–592.
- [7] R.M.F. Cardoso, et al., *Acta Cryst. D* 60 (2004) 1569–1578.
- [8] J.R. Lakowicz, *Principles of Fluorescence Spectroscopy*, Plenum Press, New York, 1983.
- [9] T. Kishi, M. Tanaka, J. Tanaka, *Bull. Chem. Soc. Japan* 50 (1977) 1171–1267.
- [10] E. Bucci, et al., *Biophys. Chem.* 32 (1988) 187–198.
- [11] S.T. Kim, et al., *Biochemistry* 30 (1991) 11262–11270.
- [12] P.S.J.R. Lakowicz, *Biochemistry* 32 (1993) 7981–7993.
- [13] D.E. Orosz, K.D. Garlid, *Anal. Biochem.* 210 (1993) 7–15.
- [14] B. Kierdaszuk, et al., *Photochem. Photobiol.* 61 (1995) 319–324.
- [15] D. Bartlett, M. Glaser, R. Welti, *Biochim. Biophys. Acta* 1328 (1997) 48–54.
- [16] X. Li, et al., *Anal. Chimica. Acta* 515 (2004) 255–260.
- [17] L.L. Hench, J. Wilson (Eds.), *An Introduction to Bioceramics*, World Scientific, New York, 1993.
- [18] A.L. Lehninger, D.L. Nelson, M.M. Fox, *Principles of Biochemistry*, 2nd ed., Worth Publishers, New York, 1993.
- [19] T. Kukubo, et al., *J. Biomed. Mater. Res.* 24 (1990) 721–734.
- [20] F.C. Giacomelli, C. Giacomelli, A. Spinelli, *J. Braz. Chem. Soc.* 15 (4) (2004) 541–547.
- [21] I. Tatischeff, et al., *C.R. Acad. Sci. Paris. Series D* 276 (1973) 1217–1220.
- [22] A.J. Pesce, C.G. Rosen, T.L. Pasby, *Fluorescence Spectroscopy: An Introduction for Biology and Medicine*, Marcel Dekker Inc., New York, 1971.
- [23] J.N. Demas, G.A. Crosby, *J. Phys. Chem.* 75 (1971) 991–1024.
- [24] M. Krieg, M.B. Srichai, R.W. Redmond, *Biochim. Biophys. Acta* 1151 (1993) 168–174.
- [25] R.F. Chen, *Analy. Lett.* 1 (1967) 35–42.
- [26] F.W. Teale, W. Weber, *Biochem. J.* 65 (1957) 476–482.
- [27] J. Strickler, R.A. Berg, *J. Chem. Phys.* 37 (1962) 814–822.
- [28] C.G. Nan, et al., *Talanta* 49 (1999) 319–330.
- [29] R.F. Steiner, E.P. Kirby, *J. Phys. Chem.* 73 (1969) 4130–4135.
- [30] B. Hichel, K.H. Schmidt, *IBID* 74 (1970) 2470–2474.
- [31] P. Cavarotta, R. Favilla, A. Mazzini, *Biochim. Biophys. Acta* 578 (1979) 541–546.
- [32] R.W. Ricci, J.M. Nesta, *J. Phys. Chem.* 80 (1976) 974–980.
- [33] S.S. Lehrer, *J. Am. Soc.* 92 (1970) 3459–3462.
- [34] J.A. Dean, *Lange's Handbook of Chemistry*, 14th ed., Mcgraw-Hill, New York, 1992.
- [35] Chem3D of CambridgeSoft Corp., V. 6.0, in press.
- [36] J.T. Edwards, *J. Chem. Educ.* 47 (1970) 261–270.
- [37] N. Sutin, *Acc. Chem. Res.* 15 (1982) 275–282.
- [38] H. Zeng, M. Sow, G. Durocher, *J. Lumin.* 62 (1994) 1–16.
- [39] P. Debye, *Trans. Electrochem. Soc.* 82 (1942) 265–271.

- [40] R.M. Fuoss, J. Am. Chem. Soc. 80 (1958) 5059–5061.
- [41] M. Eigen, Z. Phys. Chem. 1 (1954) 176–200.
- [42] I.R. Gould, S. Farid, Acc. Chem. Res. 29 (1996) 522–528.
- [43] H. Knibbe, A. Weller, Ber Bunsen-Ges: Phys. Chem. 72 (1968) 257–262.
- [44] A. Weller, Z. Phys. Chem. 130 (1982) 129–138.
- [45] J.M. Chen, T.I. Ho, C.Y. Mou, J. Phys. Chem. 94 (1990) 2889–2896.
- [46] R.A. Marcus, J. Chem. Phys. 24 (1956) 966–978.
- [47] H.S. Harned, B.B. Owen, The physical Chemistry of Electrolytic Solutions, Reinhold Publ. Corp., New York, 1943.
- [48] J. Gangopadhyay, S.C. Lahiri, Z. Phys. Chemie 215 (2001) 883–891.
- [49] I. Shehatta, A.M. Kiwan, Z. Phys. Chemie. 215 (2001) 847–865.
- [50] J. Gangopadhyay, S.C. Lahiri, Z. Phys. Chemie 215 (2001) 837–846.
- [51] A.N. Asaad, P. Krebs, Chem. Phys. Lett. 137 (1987) 553–558.
- [52] E. Lemp, A.L. Zanonco, G. Gunther, J. Photochem. Photobiol. B 65 (2001) 165–170.
- [53] H.S. Harned, A.M. Ross Jr., J. Am. Soc. 63 (1941) 1993–1999.
- [54] I. Roberts, L.P. Hammett, J. Am. Soc. 59 (1937) 1063–1070.
- [55] D.R. Lide, CRC Handbook of Chemistry and Physics, 77th ed., CRC Press, Boca Raton, Florida, 1996.
- [56] D. Rehm, A. Weller, Isr. J. Chem. 8 (1970) 259–271.
- [57] A. Weller, Z. Phys. Chem. NF 133 (1982) 93–98.
- [58] K. Kikuchi, et al., Z. Phys. Chem. NF 173 (1990) 421–424.
- [59] M.O. Iwunze, Monatsefte fur Chemie 135 (2004) 231–240.
- [60] K. Kikuchi, J. Photochem. Photobiol. A 65 (1992) 149–156.
- [61] T.N. Inada, et al., J. Photochem. Photobiol. A 137 (2000) 93–97.
- [62] K. Kikuchi, et al., Chem. Phys. Lett. 80 (1991) 403–408.